VFAST Transactions on Software Engineering
https://vfast.org/journals/index.php/VTSE@ 2024, ISSN(e): 2309-3978, ISSN(p): 2411-6246
Volume 12, Number 2, April-June 2024 *pp: 31-45*

Exploring Long-Range Order in Diblock Copolymers through Cell Dynamic Simulations

Muhammad Javed Iqbal [1*], **Inayatullah Soomro** [1], **Mumtaz Hussain Mahar** [2], **Usama Gulzar** [1]

[1]Department of Mathematics, Shah Abdul Latif University Khairpur, Pakistan; [2]Department of Computer Science, SZABIST Larkana, Sindh, Pakistan

Keywords:
Nanotechnology, Soft matter, Cell dynamic simulations, Diblock copolymer system, Numerical solution of PDEs, Computational modelling.

Journal Info:
Submitted:
April 18, 2024
Accepted:
May 26, 2024
Published:
June 2, 2024

Abstract

Soft materials have played an important role in the development of nanotechnology over the past decade. Diblock copolymer systems in these soft materials have opened up new avenues of research, introducing discoveries in experimental and theoretical research in the bulk and melt states. To this end, computer programming has advanced the simulation of soft materials through mathematical models that have enabled the prediction of novel ordered structures and morphologies from simulations on long-range order. Using this approach proved to be cost-effective and time-efficient. There are many mathematical models for predicting novel morphologies in diblock copolymer systems by computer simulation. Still, cell dynamic simulation (CDS) stands out for its efficiency and robustness in achieving long-range order. This paper presents a cell dynamic simulation model for predicting simulation results by examining flow, deformation and phase transitions within diblock copolymer systems in curvilinear coordinate systems. The paper insight into the interpretation, understanding, scope, and application of the partial differential equations involved in the model by presenting a block diagram of the CDS model with a modified algorithm. A numerically consistent CDS numerical scheme is developed. Laplacian is involved in the CDS model based on curvilinear geometries to solve regular and irregular system boundaries. Also, self-assembly, phase separation mechanism, predicted results and applications in diblock copolymer systems are highlighted. Finally, the results of the CDS model are also presented for comparison with other models.

***Correspondence author email address:** mjaved.iqbal@salu.edu.pk
DOI: 10.21015/vtse.v12i2.1795

1 Introduction

The computing can easily handle intensive tasks including numerical simulations, data analysis and optimization problems. Improves overall performance due to multiple computing units which helps to reduce computational cost. Diblock copolymer system can be overcome to predict complex novel morphologies of polymer systems at large that would not normally be possible by other computing simulations [1].

The manipulation and engineering of materials at the nanoscale is called nanotechnology, in which novel optical, electrical, and mechanical properties of materials highlight the importance of their counterparts. These features open the door to new possibilities for new and advanced technologies. Soft materials are mechanically soft and macroscopically complex materials that are easily deformed. These include polymers, liquid crystals, surfactants and colloids. Soft materials undergo thermal fluctuations over time. They are formed by interactions between intermolecular forces and kinetic properties [2–4].

The spontaneous formation of complex structures of soft materials is due to their self-assembly and phase separation system. Nanoscale control over the self-assembly system is possible due to the dominance of thermal fluctuations induced disruption over attractive interactions, which remains a challenge because many complexities are involved in fabricating defined nanostructures viable for miniature technologies [5, 6]. Monomers combine to form polymers and the covalent bonding of thermodynamically incompatible polymers of two species leads to the formation of diblock copolymer systems. Polymers are a subset of macromolecules based on monomeric chains [7].

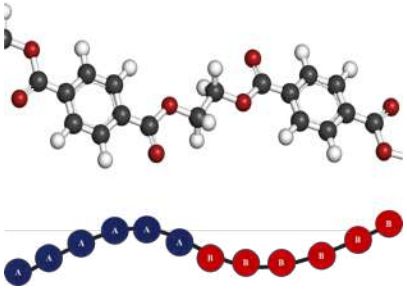

Figure 1. Chain Segment of AB-Diblock copolymer system

One type of monomeric chain is a homopolymer, and two monomers in the same chain form a copolymer. Diblock copolymer systems, Shown in Figure-1, refer to a unique and valuable class of materials in which two blocks are covalently linked and undergo microphase separation due to mutual incompatibility, which drives the self-assembly of individual polymer domains and various ordered nanostructures exist at the nanoscale level [8–11].

These nanostructures formed by self-assembly, shown in Figure 2, through microphase separation, diblock copolymers, have various applications due to their intrinsic potential, including nano structural templates, nanolithography, nano high-density storage devices, nanofabrication and nano printing, as well as nonporous membranes.

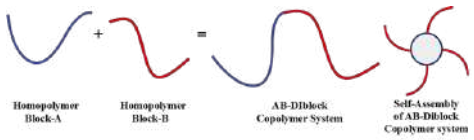

Figure 2. Self-assembly of AB-Diblock copolymer system

These nanostructures can be spherical (*S*), cylindrical (*C*) and lamellar (*L*) in structure, as shown in Figure 3. Each polymer component adapts to the conditions of the novel pattern and integrates effectively based on its properties to create additional functionality. The degree of segregation χN is inversely proportional to the temporal parameter τ. The Flory Hugin parameter χ and defined by:

$$\chi_{AB} = \frac{Z}{K_B T}\{\varepsilon_{AB} - \frac{\varepsilon_{AA} + \varepsilon_{BB}}{2}\} \quad (1)$$

χ_{AB} is an interactive parameter of the *A* and *B* block of the AB-diblock copolymer system, *Z* represents the numbers of nearest neighbouring monomers, ε_{AB}, ε_{AA} and ε_{BB} is the interactive energies associated with *A* – *A*, *A* – *B* and *B* – *B* interactions in the system respectively. The positive value of χ_{AB} means the repulsive interaction causes the macrophase separation in the system. K_B represent the Boltzmann constant, approximately $1.380 \times 10^{-23} jk^{-1}$, a ratio between the average kinetic energy *E* to absolute temperature *T*, used to explain the entropy and disorder in the system.

he average thermal translational energy is calculated by the order of K_BT, increasing proportionally to the T. The composition of a block in an AB-diblock copolymer system is expressed in volume fraction:

$$f_\alpha = \frac{N_\alpha}{N} \quad (2)$$

If $\alpha = A$ and $f_A = 0.5$, the system contains symmetric, otherwise, asymmetric blocks. The minimum value of χ_{AB} is required 10.5 to predict Lamellae morphology in Bulk. A higher χ_{AB} value leads to better block segregation and, consequently, more ordered lamellae. The higher value of N leads to stable Lamellae and exhibits a larger domain size. The value of T must be below the order-disorder transition temperature.

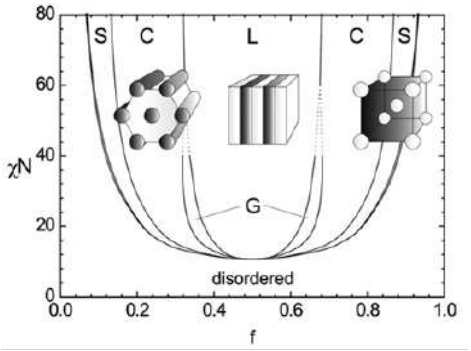

Figure 3. Emerging morphologies of AB-diblock copolymers system in Bulk

The fluctuation and frustration in the system cause the higher or lower thermal translational energy of the molecule. Temperature changes are transferred to the chains of diblock copolymers in the form of thermal energy, which counteracts the interchain attractions that drive self-assembly. In this study, novel morphologies formed by changes in temperature, changes in ordering dynamics, microphase separation mechanisms, and insights into non-equilibrium assembly control are attempted to be understood through cell dynamic simulations. Careful modulation of temperature mapping phases helps design thermally robust block copolymer applications and nanostructures [12–15].

Diblock copolymer systems have been extensively studied experimentally and theoretically over the past decades. Mathematical modelling and computer programming simulation methods have been adopted to avoid large laboratory and time costs. Factors characterizing phase behaviour, self-assembly mechanisms, morphology diagrams, domain sizes, and structural changes in soft materials are beginning to be examined over time. To investigate the nanoscale morphology in a variety of block copolymer materials, a wide range of analytical techniques have been used, including transmission electron microscopy, atomic force microscopy, small-angle X-ray, and neutron scattering. Additionally, computational modelling with methods such as self-consistent field theory, molecular dynamics and cell dynamic simulations has led to a solid molecular-level understanding of the driving forces governing microphase separation [16–22].

Block copolymer systems have been central to soft materials investigation due to their relevance for nanomanufacturing. This extensive and multidisciplinary research effort has yielded fundamental insights in theoretical sciences into how the structure, chain architecture, and influence the configuration of processing conditions is the realization of non-equilibrium assembly, interfacial behaviour, directed self-assembly, and multi-core applications for the industrial revolution. The goal of this investigation is to predict novel morphologies in diblock copolymer systems through cell dynamic simulations, with the main motivation being to develop these morphologies for long-range domains of specially designed nanodevices [23–25].

This paper includes an explanation of the cell dynamic model, the scope, and the computer simulation steps and descriptions of the tools used in the model. This research also focuses on confinement and other similar constraints to enhance the structural refinement of macromolecules to accelerate self-assembly processes to enable the elimination of defects to achieve large-scale order structures. Diblock copolymers are difficult to practically and experimentally prepare and study due to their intrinsic molecular complexity. Computational modelling provides valuable guidance for experiments by predicting and

complementing experimental research. To achieve this goal, over the years, various computational techniques have been used to understand diblock copolymer systems, investigate their dynamics, and generate novel patterns. Although limited to small time or length scales, molecular dynamics (MD) simulations exhibit fully atomistic resolution, Monte Carlo (MC) simulation methods require random sampling if large-scale thermodynamics are to be studied from MD. Use take. Similarly, viscous representations with longer time frames are used in dissipative particle dynamics (DPD) simulations and Brownian dynamics (BD) simulations. The time-dependent Ginzburg-Landau (TDGL) method with cell dynamics simulation (CDS) captures the dynamics of microphase separation by employing nonparametric free energy as well as equilibrium as a function of molecular properties. The shapes are predicted using static self-consistent field theory (SCFT). If an analysis of the dynamics of a non-equilibrium assembly is desired, dynamics self-consistent field theory (DDFT) is used instead of SCFT. The differential equations governing the microphase separation in all aspects of the simulations are directly integrated into the theoretical simulations [26–38].

Along with the above discussion, it is important to understand and motivate the reasons why the CDS model uses a mesoscale modelling approach on irregular and curvilinear geometries that compare processes of enthalpic block segregation and entropic mixing. This could examine the self-assembly of diblock copolymers using a lattice-based representation of space with the resulting discrete cell states. The use of this model provides fundamental insight into the kinetic pathways during formation and provides predictive guidance for rational material design by relying on factors such as equilibrium contours. Simulation-based prediction of long-range ordered novel morphologies has proven extremely computationally expensive in real-time and at an experimental scale with conventional serial algorithms.

It is difficult to simulate systems of experimental size and experimental timing on this model, even on modern sub-band processors. To connect the novel simulation results predicted with experimental results, it is necessary to use large simulation boxes to create a computer program that can be run simultaneously by connecting many processors in parallel and overcome the computational cost issues. In the introduction to this paper, we have described the importance of cell dynamic simulation and the background of diblock copolymer systems. In the next section, cell dynamic simulation block diagram, mathematical model and parallel computing mechanism are presented in spherical linear coordinates. Finally, a comparison of different simulation models and cell dynamic simulation is presented.

2 Cell dynamic simulation model

Cell dynamic simulation is primarily a cellular automaton modelling technique used to simulate time-discrete domains of interfacial dynamics for phase-separating systems by converting the simulation space into a cell lattice of different phases. A cell dynamic simulation model is constructed in such a way that it can understand the dynamics in the form of iterative updates of the relative interaction values of neighbouring cells. Cell-to-neighbor cell adhesion occurs, and cells coalesce to form dynamic interfaces during these stages [39, 40].

The flow chart of the CDS one-order model for the simulation of the AB-diblock copolymer system confined in curvilinear geometries is given in Figure 4. The macromolecule of the system is a covalent bond of two thermodynamically incompatible blocks of distinct homopolymers. This macromolecule is simulated based on different sets of partial differential equations involved in the system. The mechanism involved is known as a discretization of the physical space of the macromolecule. The simulation space of the lattice is divided into a discrete set of points associated with the space cell. Each cell has some specific space and small volume element. The cells involved in the system are associated with some state corresponding to phase. After converting the continuum macromolecule to a discrete set of points, discretization using finite-difference techniques in polar, cylindrical, or spherical geometries generates a numerical scheme for the Laplacian.

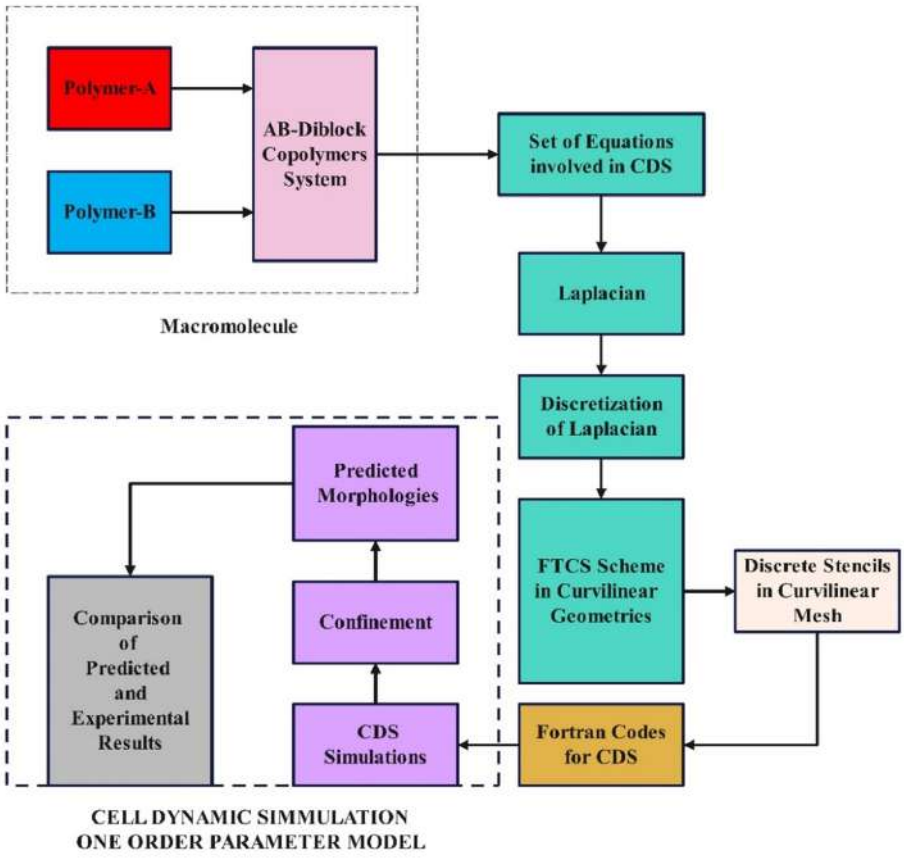

Figure 4. Cell Dynamic Simulation Model

The data files are obtained by programming the model in FORTRAN codes and running the simulation at tuning of different parameters. Dynamics in the simulation model are driven by local interactions and directions between neighbouring cells based on predefined rules. The cell-to-cell interaction energy in the system is calculated based on parameters such as interface energy for different cell states. During simulation, the total interaction energy of the system is tuned to a minimum rating to determine each new state of each cell at different time steps, thereby encouraging phase separation by each cell being influenced by the majority state of its neighbouring cells.

This indicates that random fluctuations are incorporated to simulate the effects of temperature on different variables. The system progresses in time with many iterative updates, allowing complex patterns to emerge at large scales and microstructures to evolve. System properties are compared to experimental observations by analyzing the domain size, distribution, coarsening rate, and comparative analysis. The CDS model is used for the simulation of any system where it is desired to examine the transitional insight between any two subsystems within the system. These include insight into metal alloy phase separation, testing the mixing of two different immiscible fluid components, and understanding the formation of different order structures with time evaluation in diblock polymer systems [41, 42].

3 Cell dynamic simulation under curvilinear confinement

Macromolecule of AB-diblock copolymer system having volume V, having two blocks A and B with chain length N_A and N_B respectively. A polymer containing f_α, $\alpha = A$ or $\alpha = B$ monomers with $f_\alpha z$ statistical segment length and scale length $ln^{\frac{1}{2}}$ (l is kahn length). The local volume fraction of polymers is:

$$\phi_\alpha = \frac{1}{\rho_0} \sum_{i=1}^{N} \int_0^{f_\alpha} d\zeta \delta\{r - r_i^\alpha(\zeta)\} \tag{3}$$

Here $0 \leq \zeta \leq N = N_A + N_B$. This is a theoretical framework to understand the volume fraction of any block in a diblock copolymer system about self-assembly insight. The ϕ_α represent the total volume of any block in the system. ρ_0 is a reference density of melt connectivity of a homogeneous mixture of α blocks. The monomer chain has N number of molecules. $\sum_{i=1}^{N}$ indicates the evaluation sum of every i^{th} molecule. The integration limits 0 to f_α indicate the average time spent characterized with f_α block. δ is a Dirac delta function associated with a specific space point, used for incompressibility constraint. r is the position of molecule concerning the $r_i^\alpha(\zeta)$ position of the i^{th} molecule of α blocks. $r_i^\alpha(\zeta)$ explains the chain confoemations [43, 44].

When simulating diblock polymers in the CDS model, the local and global volumes are taken into account in the CDS model. The CDS model uses local cells of lattice to represent small-scale structural fluctuations in the global volume to elucidate the block constraints of the self-assembly dynamics. The local volume in the simulation grid represents an individual cell or lattice site. Each cell contains a local volume of A-block, ϕ_A and the local volume of B-block, ϕ_B . The global volume in the CDS model refers to the collective volume of the entire simulation domain and region of all cells. When aggregating the global volume, the frequency of cells, the share of A-block or B-block in all cells and the total volume of each block are conserved. Local volumes may vary between cells and may be of the same volume, but the volume of the global mixture remains constant and conserved. Local volumes produce microphase separation over time under the influence of global compositional constraints.

The order parameter quantifies the deviation of the amount of homogeneity at the spatial scale. Leiber [45] introduced the concept of the order parameter as the "spatial average of the product of the local composition fluctuations of the different monomers blocks" in the diblock copolymer system. The order parameter measures the phase separation between two different polymer blocks due to inhomogeneity. It also quantifies the degree of segregation in these different blocks. The range of this order parameter ψ in bulk is $0 < \psi < 1$. If $\psi = 0$, the monomers are randomly distributed in a completely disordered state without any segregation. If $\psi = 1$, the monomers are in a perfectly ordered state with complete segregation of different monomers in distinct domains or phases.

Experimentally, the order parameter is achieved by different techniques including small angle X-ray scattering (SAXS) [46], neutron scattering [47] and transmission electron microscopy (TEM) [48]. Theoretically or computationally, it is obtained by different computational techniques described earlier. In this paper, the focus is to obtain this order parameter by cell dynamic simulation. In simulation of diblock copolymer melt the range of order parameter is $-0.5 < \psi < +0.5$. In the simulation process, the order parameter is the same as the tuning of χN in SCFT bulk phase diagram shown in Figure 2. The order parameter ψ is influenced by the Flory Hugin parameter χ, volume fraction f_α. The generation of equilibrium phases is due to χN as a function of f_α, morphologies of equilibrium phases are obtained as a function of system parameters. The high degree of macrophase separation is due to the high value of the order parameter, proportional to the high value of χN. The choice of order parameter enables potentially predictable morphologies suitable for nanolithography, drug delivery and membrane separation media [49].

In the discrete lattice of the diblock copolymer system, the order parameter of the i^{th} cell of the diblock copolymer system at the time t is represented by is $\psi(i, t)$

$$\psi = \phi_A - \phi_B + (1 - 2f). \tag{4}$$

Equation (4) explains the computational asymmetry in the CDS model. The order parameter determines the self-interaction interface between different blocks and has a good influence on the simulated self-assembly of the AB diblock copolymer system. ϕ_A and ϕ_B are local volume fractions of different chemical species' A and B blocks, respectively as given in (3). The local volume fraction derives microphase separation employing block imbalance in block imbalance in i^{th} cell. f is a global volume and $(1 - 2f)$ is a composition-dependent term. If $\phi_A = \phi_B$ for a mixed state, the order parameter is defined by the term $(1 - 2f)$ in this disordered state. The cell interaction guidelines, the cell with $\psi > 0$, favours the A-block and the cell with $\psi < 0$, favours the B-block [50].

The order parameter quantifies the deviation of the local region from the ideal mixed condition and f is:

$$f = \frac{N_A}{N_A + N_B} \tag{5}$$

The continuity equation has an important role in studying the CDS model. It explains the rate of change of the order parameter in the form of divergence of its flux $j(r, t)$. Continuity equations and conservation systems aim to account for changes in dynamics. The conservation expression for the "sum" of kinetic fluctuations during phase separation is represented by an order parameter. In practice, the propagation of the order parameter from the higher regions to the lower regions depends on the continuity equation. The continuity equation mathematically imposes a constraint on the order parameter to obey the time evolution of the propagation dynamics. The flux $j(r, t)$ determines the relaxation or diffusion of the order parameter. Updates of the continuity equation are spatially and temporally resolved during the simulation, helping to ensure that the initial fluctuations behave through dynamics rather than the sudden emergence of spontaneous transport [51].

The rate of change of the order parameter $\frac{\partial \psi(r,t)}{\partial t}$ is given as a continuity equation:

$$\frac{\partial \psi(r, t)}{\partial t} = -\nabla j(r, t). \tag{6}$$

The conservation of probability density with change in time is represented in (6). The flux is associated with spatial location r over time t. The negative sign in $-\nabla j(r, t)$ is the probabilistic measure of the increasing net flow.

The flux $j(r, t)$ is linearly connected to the local chemical potential:

$$j(r, t) = -M\nabla\mu(r, t). \tag{7}$$

This is a relation between flux $j(r, t)$, mobility constant of transport M and the negative gradient of the chemical potential μ. The relation between the flux and the chemical potential links the local thermodynamic driving factors to the structural flux, regulating the dynamics of the actual non-equilibrium phase separation. The flux $j(r, t)$ of any block at the location r during time t describes the quantity and direction of transport flow. From this relation, the transport kinetics are established via the order parameter to drive the self-assembly in the CDS model, which restricts the classical dissolution kinetics to minimize the free energy described by the local chemical potential μ. The negative sign indicates the flow direction is towards decreasing chemical potential (the region with high free energy to the region with low free energy).

The chemical potential of system is influenced by blocks preferential interactions, confinement effect and abstract fields. The chemical potential μ is given by the functional derivative of the free energy in the following way:

$$\mu(r, t) = \frac{\delta F[\psi]}{\delta \psi}. \tag{8}$$

In the context of the CDS model, this equation describes the relationship between the chemical potential field of a block $\mu(r, t)$ at r location and time t in the system, order parameter ψ as the local preference field and the free energy functional $F[\psi]$ within the model. A free energy functional V refers to a representative function that captures the total energy of a system as a function of other relevant fields in the model. It depends upon order parameter field. $F[\psi]]$ incorporates entropy of mixing, energy interaction among blocks and energy required to interface among different phases. In this context, $F[\psi]$ represent the overall free energy of the system depending on the simulation domain. $\frac{\delta F[\psi]}{\delta \psi}$ is a variational derivative

determining the response of free energy towards variation in ψ. It is clear from the equation that μ guides reorienting ψ toward equilibrium during oscillation. At the same time, it directly links thermodynamics and transport kinetics in CDS models by equating ? to the variable derivative. The Cahn-Hilliard-Cook (CHC) is used to describe phase separation in the CDS model. The CHC equation is essentially a combination of two equations, the Cahn-Hillard and the Cook model, which aim to describe the behaviour of diffusion as a gradient with dynamics. The time evolution of the order parameter in the CHC equation is related to the gradient of the chemical potential by $\frac{\delta\psi}{\delta t} = \nabla.M\nabla\mu$. This proves the connection between thermodynamics and transport kinetics. The equation accounts for diffusion updates over time to the order parameter during self-assembly during simulation. To do this it has to deal with thermodynamic driving forces and non-equilibrium concentration fluctuations [52, 53].

The Cahn-Hilliard-Cook (CHC) equation describes the order parameter's time evolution:

$$\frac{\partial\psi}{\partial t} = M\nabla^2\left(\frac{\delta F[\psi]}{\delta\psi}\right) + \eta\xi(r,t). \tag{9}$$

The equations of the CDS model combine relaxation dynamics and chemical driving forces to adjust free energy and fundamental thermodynamics with a noise term added to account for fluctuations. The equation (9) is used in simulations to understand phase separation phenomena. The value of the mobility constant is set at $M = 1$ to set the maximum rate of diffusion transport corresponding to the time scale, $\eta\xi(r,t)$ is stochastic noise η is the noise amplitude and $\xi(r,t)$ is a stochastic noise field normally distributed. The presence of the noise term in the equation is not programmed into the model as it does not have a substantial impact on the simulation results. However, it is included in the equation of the original model for the sake of retaining its completeness and original form. The Laplacian operator ∇^2 [54] is used here that act as a gradient for the next term. The inclusion of a noise term introduces physically realistic fluctuations near the critical points where the ordered domain just begins to develop, the absence of noise indicates a steep drop in free energy. Variation in η disrupts the real fluctuations. The large value of η indicates larger response fluctuations and system frustration. Thermal fluctuations are of great importance in the simulation of material systems to exhibit microstructural evolution and phase transitions. These fluctuations affect the overall behaviour of the system as they cause random variations in the order parameter. Dividing the free energy functional with the product of Boltzmann constant with temperature *KT* gives us a dimensionless free energy functional that is consistent with the thermodynamics of computational modelling. *KT* sets the thermal energy at a given local temperature. This assures us that the equilibrium properties and dynamic behaviour of the system can now be easily obtained through the equations, helping us to gain insight into the effects of both energetic contributions and thermal fluctuations [55, 56]. The free energy functional $\frac{F[\psi(r)]}{KT}$ is represented by the equation:

$$F[\psi(r)] = \int dr\left[H(\psi) + \frac{D}{2}|\nabla\psi|^2\right] \tag{10}$$

$$+\left(\frac{B}{2}\right)\int dr' G(r-r')\psi(r)\psi(r'). \tag{11}$$

The equation has two terms, first is for short range and second is for long range interaction. The diffusion coefficient is presented by D and B introduced free energy-dependent chain length. is a green function. The Green's function $G(r-r')$ is a pair correlation function, with this function we estimate the probability density of finding a particle at a position r given that the other particle is at a position r'. This provides information about the spatial arrangements and correlations between particles in the system. $(r-r')$ is a difference vector between two particles that specifies the distance and direction from one particle to the other. $G(r-r')$ is used to analyze structural properties and interactions in the CDS model and gives us the ability to understand the distribution and arrangement of particles as well as the degree of clustering or segregation within the system. H(?) is free energy [57]:

$$H[\psi] = \left[-\frac{\tau}{2} + \frac{A}{2}(1-2f)^2\right]\psi^2 + \frac{v}{3}(1-2f)\psi^3 + \left(\frac{u}{4}\right)\psi^4 \tag{12}$$

Where *A*, *u* and *v* are phenomenological constants. Ohta and Kawasaki [58], expressed *D*, *B* and in terms

of f, N, b and . N is the degree of polymerization and b is the length of the segment. Flory-Huggin's parameter χ is inversely proportional to temperature.

$$\tau = A(1-2f)^2 - \tau' \tag{13}$$

and

$$\tau' = -(N\chi - \frac{s(f)}{4f^2(1-f)^2}) \tag{14}$$

$$D = \frac{b^2}{48f}(\frac{1}{1-f}) \tag{15}$$

$$B = (\frac{3}{2Nbf(1-f)})^2 \tag{16}$$

$s(f)$ is the function used to maintain χ across compositions. If $s(f) > 0$, it favours phase separation and if $(f) < 0$, it favours mixing. For better stability, Oono and Puri [59], suggest $H(\psi)$ in another way.

$$H(\psi) = -Aln(cosh\psi) + \frac{1}{2}(\psi)^2 \tag{17}$$

Now final CDS equation is given as:

$$\frac{\partial\psi}{\partial t} + \nabla.(\upsilon\psi) = \eta\xi(r,t) + M\nabla^2\frac{\delta F[\psi]}{\delta\psi} \tag{18}$$

The numerical evolution of the CDS model (17) for order parameters is given as:

$$\begin{aligned}\psi(\mathbf{n},t+1) &= \psi(\mathbf{n},t) - \{\langle\langle\Gamma(\mathbf{n},t)\rangle\rangle - \Gamma(\mathbf{n},t)\} \\ &\quad +B\psi(\mathbf{n},t) - \eta\xi(\mathbf{n},t).\end{aligned} \tag{19}$$

where

$$\Gamma(\mathbf{n},t) = g(\psi(\mathbf{n},t)) - \psi(\mathbf{n},t+1) + D\{\langle\langle\psi(\mathbf{n},t)\rangle\rangle - \psi(\mathbf{n},t)\} \tag{20}$$

and

$$g(\psi) = \psi[1 - A(1-2f)^2 + \tau] + \psi^2(1-2f)\upsilon - \psi^3 u \tag{21}$$

At lattice point $\mathbf{n} = (n_x, n_y, n_z)$ and time t, the order parameter $\psi(\mathbf{n},t)$ representing the composition. $\psi(\mathbf{n},t+1)$ is updated order parameter after one time step $(t+1)$.$\Gamma(\mathbf{n},t)$ is the gradient of chemical potential at a lattice point $\mathbf{n}$ and time t. $\langle\langle\Gamma(\mathbf{n},t)\rangle\rangle$ is the spatial average of $\psi(\mathbf{n},t+1)$. The difference $\langle\langle\Gamma(\mathbf{n},t)\rangle\rangle - \Gamma(\mathbf{n},t)$ represent a driving force to account for composition change. This can be represented by $\langle\langle\Gamma(\mathbf{X})\rangle\rangle - \Gamma(\mathbf{X})$ to describe isotropized discrete Laplacian in rectangular, polar, cylindrical and spherical mesh for free energy functional $\Gamma(\mathbf{n},t)$ at Δt steps of the order parameter $\psi(i,t)$, where $\mathbf{n} = (n_r, n_\theta)$ in a polar coordinate system, $\mathbf{n} = (n_r, n_\theta, n_z)$ in a cylindrical coordinate system and $\mathbf{n} = (n_\rho, n_\theta, n_\phi)$ in a spherical coordinate system [60]. Confinement is enforced by limiting the simulation parameters in the CDS model of the diblock copolymer system. In this way, novel morphologies with new dimensions of self-assembly are realized upon the addition of frustration to the system whose predictions are compared with experimental morphologies to prove the validity of the model and simulation patterns. In case of confinement:

$$\begin{aligned}\Gamma(\mathbf{n},t) &= g(\psi(\mathbf{n},t)) - \psi(\mathbf{n},t) \\ &\quad +D\{\langle\langle\psi(\mathbf{n},t)\rangle\rangle - \psi(\mathbf{n},t)\} + S_i r\end{aligned} \tag{22}$$

Here $S_i r) = h_i \times \phi_i \times \delta_{n_r=1 or n_r=N_r}$ are the boundary conditions. The strength of the mutual interaction of walls and blocks is h_i. The Kronecker Delta is given as:

$$\delta = \begin{cases} 1 & if \quad A = B \\ 0 & if \quad A \neq B \end{cases} \tag{23}$$

3.1 The Laplacian in Cartesian mesh.

$$\nabla^2\psi = \psi_{xx} + \psi_{yy} \tag{24}$$

3.2 The Laplacian in Polar mesh.

$$\nabla^2\psi = \psi_{rr} + \frac{1}{r}\psi r + \frac{1}{r^2}\psi_{\theta\theta} \tag{25}$$

The boundary conditions are constraints to the angular grid $0 \leq \theta \leq 2\pi$ with $\theta_j = j\Delta\theta$ for $j = 1, 2, 3, \ldots, n_\theta$ and radial grid $r_a \leq r \leq r_b$ with $r_i = r_a + i\Delta r$ for $i = 1, 2, 3, \ldots, n_r$

3.3 The Laplacian in Cylindrical mesh.

$$\nabla^2\psi = \psi_{rr} + \frac{1}{r}\psi r + \frac{1}{r^2}\psi_{\theta\theta} + \psi_{zz} \tag{26}$$

The boundary conditions are constraints to the angular grid $0 \leq \theta \leq 2\pi$ with $\theta_j = j\Delta\theta$ for $j = 1, 2, 3, \ldots, n_\theta$ and radial grid $r_a \leq r \leq r_b$ with $r_i = r_a + i\Delta r$ for $i = 1, 2, 3, \ldots, n_r$ and azimuth grid $0 \leq z \leq z_h$ for $k = 1, 2, 3, \ldots, n_h$ and azimuth grid $k = 1, 2, 3, \ldots, n_h$.

3.4 The Laplacian in Spherical mesh.

$$\nabla^2\psi = \psi_{rr} + \frac{2}{r}\psi r + \frac{1}{r^2}\psi_{\theta\theta} + \frac{cot\theta}{r^2}\psi_{\theta} + \frac{cosec^2\theta}{r^2}\psi_{\phi\phi} \quad (27)$$

The boundary conditions are constraints to the angular grid $0 \leq \theta \leq 2\pi$ with $\theta_j = j\Delta\theta$ for $j = 1, 2, 3, \ldots, n_\theta$ and radial grid $r_a \leq r \leq r_b$ with $r_i = r_a + i\Delta r$ for $i = 1, 2, 3, \ldots, n_r$ and azimuth grid $0 \leq z \leq z_h$ for $k = 1, 2, 3, \ldots, n_h$ and $0 \leq \phi \leq 2\pi$.

4 Parallel Computing

In the computing method, a local decomposition method has been adopted in parallel using IFORT programming, which reduces the computational cost and the simulation of the novel pattern has been achieved at a better speed. For this purpose, the spatial decomposition method is applied.

4.1 The spatial decomposition method

Local decomposition is a valuable technique in parallel computing in which computations are performed by dividing the computational domain into subdomains and assigning a processor or computing unit to work on a specific region. In this method, each processor is assigned a specific task and the overall local decomposition method improves the computations and also simplifies the load balancing. The spatial decomposition method enables complex cell dynamic simulations to be run with greater confidence and speed and helps to control computational costs. The circular computing domain is divided into the kth subdomains of concentric circles during the discretization as shown in Figure 5. Each circular grid is associated with a different processor. The processors are linked together in a parallel network. Each processor is associated with communication with each other. Better communication is achieved by a Message Passing Interface (MPI) in which processes of different processors are mapped to a two-dimensional topological interface for discretization in the polar grid and mapped to a three-dimensional topological interface for discretization in the cylindrical and spherical grid. The computer simulation with SCFT needs global data exchange due to FFT algorithms but the CDS model does not need it due to its simplicity. The

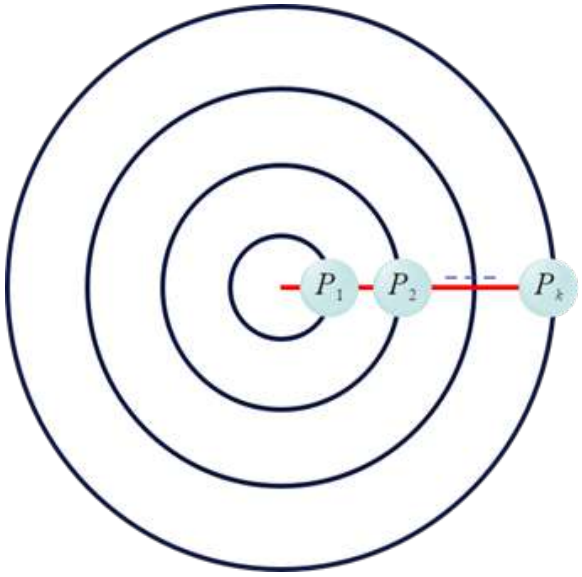

Figure 5. Partition of polar coordinate system for different processors using spatial decomposition technique.

CDS algorithm according to the above discussion is described as under [61].

Step 1:

MPI Initialization
Initialization of the value of (n,0) on different processors.
Define MPI data type

Step 2:
DO t=1, total time
Exchange boundaries of the (n,t-1)
DO n in 2-D subdomains (for two dimensions) or DO n in 3-D subdomains (for two dimensions)
Computing map function g(n,t) using equation (20)
Update boundary conditions of g(n,t)
Compute density functions (n,t) using equation (18)
ENDDO
ENDDO

Step 3:
Parallel output.

5 Applications of the CDS Model

5.1 Diblock copolymers Confined in circular annular pore

A circular forming system with and without attractive walls in circular annular pores is presented by Soomro et al. [62]. The simulation is done with the CDS model while the stencil of isotropic Laplacian is constructed by the finite difference method in the polar coordinate system. Iqbal et al. [63] presented a lamellae-forming system by using neutral and attractive walls in a polar mesh system.

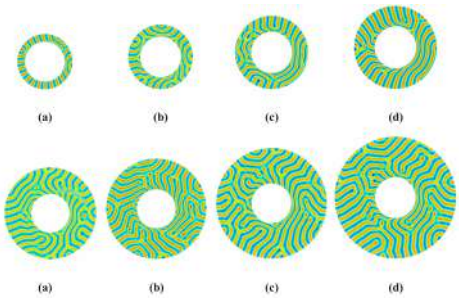

Figure 6. Lamellae forming system in annular circular pore with neutral walls in CDS model

The output results of the diblock copolymer system by the CDS model are presented with the neutral walls in Figure 6 and with confined attractive walls in Figure 7. The simulation is done for a symmetric diblock copolymer system at 1000000-time steps using cell dynamic simulation after constructing an isometric nine-point stencil of Laplacian in the polar coordinate system.

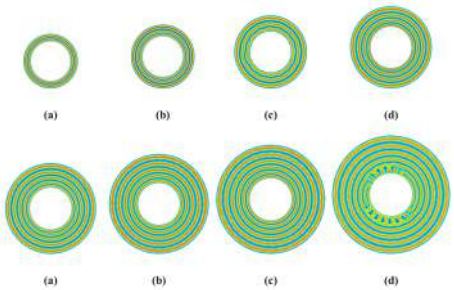

Figure 7. Lamellae forming system in annular circular pore with attractive walls in CDS model

A spherical forming system is also investigated by Javed et al. [64] with the CDS model in polar geometry by using attractive walls, shown in Figures 8 and 9. The simulation is done at 1000000-time steps using cell dynamic simulation after constructing a nine-point stencil of Laplacian in the polar coordinate system.

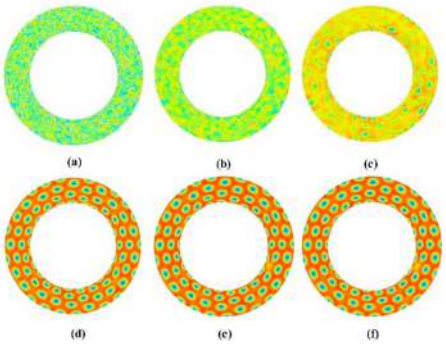

Figure 8. Spherical forming system (with time steps)in annular circular pore with neutral walls in CDS model

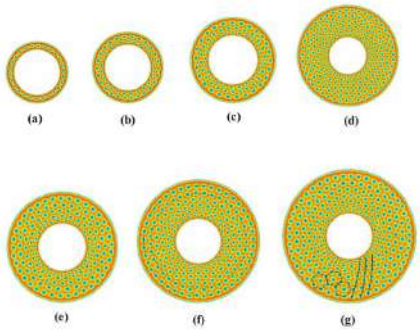

Figure 9. Spherical forming system in annular circular pore with attractive walls in CDS model

6 Comparison of the CDS model and other models

In Figure 10, a comparison of predicted studies with cell dynamic simulations with other simulation models is presented.

Lamellae morphologies1 (a), 1(b), spherical morphologies 2(a), 1(b) are obtained by the CDS model and 1(c) pattern is obtained by Monte-Carlo simulation [65], 1(d) pattern are obtained by Molecular Dynamic simulations [66] and 2(a), 2(b) patterns are obtained by Dissipative Particle Dynamics simulation model [67]. The comparison is evident that the cell dynamic

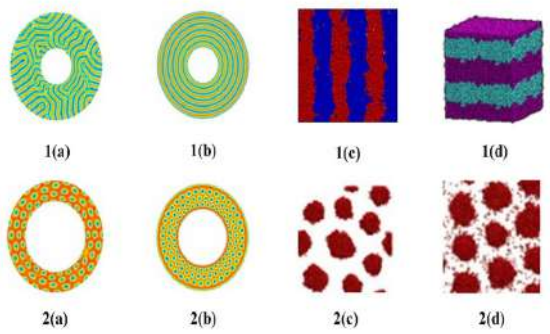

Figure 10. Comparison of predicted structures with the CDS model with other models

simulation model is more efficient, more consistent than other simulation models for the prediction of long-range order morphologies.

7 Conclusion

In this paper, cell dynamic simulation model is investigated for soft material consisting of a diblock copolymer system with essential order structures and novel morphologies for potential nanotechnology applications using different Laplacian-dominated mesh systems. The method to study the self-assembly of copolymer systems in confinement arrangements has been investigated. A model algorithm schematic diagram is presented to understand the model's insights. The set of equations involved in the model is described with clarity and justification. The Laplacian involved in the model is presented for different coordinate systems for regular and irregular boundaries. The role of Laplacian is discussed to operate cell dynamic simulation in polar, cylindrical and spherical coordinate systems with periodic and reflective boundary conditions. Validation of the model is also evaluated for its applicability to irregular boundaries and the applicability of the model to heterogeneous systems. The study emphasises the efficient role of parallel computing in the simulation of the CDS model. The spatial decomposition method and Message Passing Interface (MPI) enables CDS model more efficient and cost management model than the other simulation models.

Author Contributions

Muhammad Javed Iqbal: Conceptualization, Methodology, Software, Data curation, Writing- Original draft preparation. **Inayatullah Soomro**: Supervision, Validation..**Mumtaz Ahmad Mahr**: Visualization. **Usama Gulzar**: Writing- Reviewing and Editing

Compliance with Ethical Standards

No conflict of Interest

Funding Information

No Funding.

References

[1] X. Guo, M. Pinna, and A. V. Zvelindovsky, "Parallel algorithm for cell dynamics simulation of block copolymers," *Macromolecular Theory and Simulations*, vol. 16, no. 9, pp. 779–784, 2007.

[2] M. Doi, *Soft matter physics*. Oxford University Press, USA, 2013.

[3] S. U. Egelhaaf, X. Mao, M. Dijkstra, D. J. Pine, S. K. Kumar, M. Aubin-Tam, and G. Koenderink, "Soft matter roadmap," *JPhys Materials*, vol. 7, 2024.

[4] T. Shimizu, W. Ding, and N. Kameta, "Soft-matter nanotubes: a platform for diverse functions and applications," *Chemical reviews*, vol. 120, no. 4, pp. 2347–2407, 2020.

[5] D. Newberry, "The history of nanoscience and nanotechnology," in *Nanotechnology Past and Present: Leading to Science, Engineering, and Technology*, pp. 13–22, Springer, 2020.

[6] S. Bayda, M. Adeel, T. Tuccinardi, M. Cordani, and F. Rizzolio, "The history of nanoscience and nanotechnology: from chemical–physical applications to nanomedicine," *Molecules*, vol. 25, no. 1, p. 112, 2019.

[7] K. Spychalska, D. Zając, S. Baluta, K. Halicka, and J. Cabaj, "Functional polymers structures for (bio) sensing application—a review," *Polymers*, vol. 12, no. 5, p. 1154, 2020.

[8] C. K. Wong, X. Qiang, A. H. Müller, and A. H. Gröschel, "Self-assembly of block copolymers into internally ordered microparticles," *Progress in Polymer Science*, vol. 102, p. 101211, 2020.

[9] D. A. Filatov and E. N. Govorun, "Microphase separation in the melts of diblock copolymers with amphiphilic blocks," *Soft Matter*, vol. 17, no. 1, pp. 90–101, 2021.

[10] J. G. Werner, H. Lee, U. Wiesner, and D. A. Weitz, "Ordered mesoporous microcapsules from double emulsion confined block copolymer self-assembly," *ACS nano*, vol. 15, no. 2, pp. 3490–3499, 2021.

[11] J. Xie and A.-C. Shi, "Phase behavior of binary blends of diblock copolymers: Progress and opportunities," *Langmuir*, vol. 39, no. 33, pp. 11491–11509, 2023.

[12] E. E. Abdo, L. S. Grundy, M. D. Galluzzo, W. S. Loo, A. Y. Fong, C. J. Takacs, and N. P. Balsara, "Cylinder-gyroid phase transition in a block copolymer electrolyte induced by ionic current," *Macromolecules*, vol. 57, no. 2, pp. 503–513, 2024.

[13] H. Lee, J. Kim, and M. J. Park, "Exploration of complex nanostructures in block copolymers," *Physical Review Materials*, vol. 8, no. 2, p. 020302, 2024.

[14] W. He, F. Wang, Y. Qiang, Y. Pan, W. Li, and M. Liu, "Asymmetric binary spherical phases self-assembled by mixing ab diblock/abc triblock copolymers," *Macromolecules*, vol. 56, no. 2, pp. 719–729, 2023.

[15] J. Xie, C. T. Lai, and A.-C. Shi, "Regulating the self-assembly of ab/cd diblock copolymer blends via secondary interactions," *Journal of Polymer Science*, vol. 62, no. 4, pp. 716–732, 2024.

[16] R. Egerton, M. Hayashida, and M. Malac, "Transmission electron microscopy of thick polymer and biological specimens," *Micron*, vol. 169, p. 103449, 2023.

[17] H. Zhao, Y. Zhu, H. Ye, Y. He, H. Li, Y. Sun, F. Yang, and R. Wang, "Atomic-scale structure dynamics of nanocrystals revealed by in situ and environmental transmission electron microscopy," *Advanced Materials*, vol. 35, no. 50, p. 2206911, 2023.

[18] A. C. Dumitru and M. Koehler, "Recent advances in the application of atomic force microscopy to structural biology," *Journal of Structural Biology*, p. 107963, 2023.

[19] T. Sumikama, "Computation of topographic and three-dimensional atomic force microscopy images of biopolymers by calculating forces," *Biophysical Reviews*, vol. 15, no. 6, pp. 2059–2064, 2023.

[20] A. Romo-Uribe, "Light scattering, x-ray scattering, and microscopy studies of nanoscale polymer-based coatings," in *Polymer-Based Nanoscale Materials for Surface Coatings*, pp. 323–347, Elsevier, 2023.

[21] X. Yu, Y. Cheng, Y. Li, F. Polo-Garzon, J. Liu, E. Mamontov, M. Li, D. Lennon, S. F. Parker, A. J. Ramirez-Cuesta, *et al.*, "Neutron scattering studies of heterogeneous catalysis," *Chemical Reviews*, vol. 123, no. 13, pp. 8638–8700, 2023.

[22] T. Chen, Y. Zhang, S. Xiao, D. Yao, W. Jiang, and H. Liang, "Catalytic assembly of symmetric diblock copolymers in a thin film: a dissipative particle dynamics simulation study," *Physical Chemistry Chemical Physics*, vol. 25, no. 14, pp. 9779–9784, 2023.

[23] L. Xiang, Q. Li, C. Li, Q. Yang, F. Xu, and Y. Mai, "Block copolymer self-assembly directed synthesis of porous materials with ordered bicontinuous structures and their potential applications," *Advanced Materials*, vol. 35, no. 5, p. 2207684, 2023.

[24] L. Xiang, Q. Li, C. Li, Q. Yang, F. Xu, and Y. Mai, "Block copolymer self-assembly directed synthesis of porous materials with ordered bicontinuous structures and their potential applications," *Advanced Materials*, vol. 35, no. 5, p. 2207684, 2023.

[25] N. Politakos and A. Avgeropoulos, "Advances and applications of block copolymers," *Polymers*, vol. 15, no. 13, p. 2930, 2023.

[26] X. Feng, N. Yan, J. Jin, and W. Jiang, "Disassembly of amphiphilic ab block copolymer vesicles in selective solvents: A molecular dynamics simulation study," *Macromolecules*, vol. 56, no. 6, pp. 2560–2567, 2023.

[27] T. P. Lodge, C. L. Seitzinger, S. C. Seeger, S. Yang, S. Gupta, and K. D. Dorfman, "Dynamics and equilibration mechanisms in block copolymer particles," *ACS polymers Au*, vol. 2, no. 6, pp. 397–416, 2022.

[28] X. Guang-hai, S. Yu-han, C. Jie, H. Yuan-yuan, and F. Juan-juan, "Monte carlo simulation of the self-assembly behavior of cyclic diblock copolymers under soft confinement," *POLYMER BULLETIN*, vol. 37, no. 4, pp. 532–542, 2024.

[29] Y. Guo, W. Luo, J. Zhang, and W. Hu, "Dynamic monte carlo simulations of strain-induced crystallization in multiblock copolymers: effects of microphase separation," *Polymer*, vol. 264, p. 125512, 2023.

[30] L. Lan-ting, L. En-tian, H. Yuan-yuan, Z. Gui-yan, H. Yue-xin, H. Xiang-yan, F. Juan-juan, X. Man, and C. Jie, "Computer simulation of self-assembly behavior of cyclic symmetric diblock copolymers in thin film," *POLYMER BULLETIN*, vol. 36, no. 3, pp. 366–375, 2023.

[31] D. Liu, H. Bo, Y. Lin, D. Li, Z. Zhang, and S. Li, "Dissipative particle dynamics study on the interfacial structure and tension for polymer blends of different copolymer chemical composition distributions," *Fluid Phase Equilibria*, vol. 564, p. 113598, 2023.

[32] Y. Guo, "Dissipative particle dynamic simulation on self-assembly of symmetric cbabc pentablock terpolymers in solution," *Materials*, vol. 16, no. 23, p. 7273, 2023.

[33] A. A. Gavrilov, Y. V. Kudryavtsev, and A. V. Chertovich, "Phase diagrams of block copolymer melts by dissipative particle dynamics simulations," *The Journal of chemical physics*, vol. 139, no. 22, 2013.

[34] L.-S. Zhang, "Long-range ordered nanostructures of assembling macromolecules via rational design of kinetic pathways: a computational perspective," *Chinese Journal of Polymer Science*, vol. 41, no. 9, pp. 1318–1328, 2023.

[35] J. Diaz, M. Pinna, A. V. Zvelindovsky, and I. Pagonabarraga, "Nematic ordering of anisotropic nanoparticles in block copolymers," *Advanced Theory and Simulations*, vol. 5, no. 1, p. 2100433, 2022.

[36] J. He and Q. Wang, "Frank–kasper phases of diblock copolymer melts: Self-consistent field results of two commonly used models," *Polymers*, vol. 16, no. 3, p. 372, 2024.

[37] B. R. Magruder and K. D. Dorfman, *Theory of Block Polymer Self-Assembly*. American Chemical Society, 2024.

[38] P. Chen and K. D. Dorfman, "Gaming self-consistent field theory: Generative block polymer phase discovery," *Proceedings of the National Academy of Sciences*, vol. 120, no. 45, p. e2308698120, 2023.

[39] J. A. Stevens, F. Grünewald, P. M. van Tilburg, M. König, B. R. Gilbert, T. A. Brier, Z. R. Thornburg, Z. Luthey-Schulten, and S. J. Marrink, "Molecular dynamics simulation of an entire cell," *Frontiers in Chemistry*, vol. 11, p. 1106495, 2023.

[40] M. Serral, M. Pinna, A. V. Zvelindovsky, and J. B. Avalos, "Cell dynamics simulations of sphere-forming diblock copolymers in thin films on chemically patterned substrates," *Macromolecules*, vol. 49, no. 3, pp. 1079–1092, 2016.

[41] J. Diaz, M. Pinna, A. V. Zvelindovsky, A. Asta, and I. Pagonabarraga, "Cell dynamic simulations of diblock copolymer/colloid systems," *Macromolecular Theory and Simulations*, vol. 26, no. 1, p. 1600050, 2017.

[42] S. Ren and I. Hamley, "Cell dynamics simulations of microphase separation in block copolymers," *Macromolecules*, vol. 34, no. 1, pp. 116–126, 2001.

[43] M. Laradji, A.-C. Shi, J. Noolandi, and R. C. Desai, "Stability of ordered phases in diblock copolymer melts," *Macromolecules*, vol. 30, no. 11, pp. 3242–3255, 1997.

[44] T. Ohta and K. Kawasaki, "Equilibrium morphology of block copolymer melts," *Macromolecules*, vol. 19, no. 10, pp. 2621–2632, 1986.

[45] L. Leibler, "Theory of microphase separation in block copolymers," *Macromolecules*, vol. 13, no. 6, pp. 1602–1617, 1980.

[46] R. Chen, Y. Song, Z. Wang, H. Ji, Z. Du, Q. Ma, Y. Yang, X. Liu, N. Li, and Y. Sun, "Developments in small-angle x-ray scattering (saxs) for characterizing the structure of surfactant-macromolecule interactions and their complex," *International Journal of Biological Macromolecules*, p. 126288, 2023.

[47] R. Egerton, M. Hayashida, and M. Malac, "Transmission electron microscopy of thick polymer and biological specimens," *Micron*, vol. 169, p. 103449, 2023.

[48] W. Langel, "Introduction to neutron scattering," *ChemTexts*, vol. 9, no. 4, p. 12, 2023.

[49] R. Nisticò, "Block copolymers for designing nanostructured porous coatings," *Beilstein journal of nanotechnology*, vol. 9, no. 1, pp. 2332–2344, 2018.

[50] M. Pinna and A. Zvelindovsky, "Large scale simulation of block copolymers with cell dynamics," *The European Physical Journal B*, vol. 85, pp. 1–18, 2012.

[51] J. Diaz, M. Pinna, A. V. Zvelindovsky, and I. Pagonabarraga, "Phase behavior of block copolymer nanocomposite systems," *Advanced Theory and Simulations*, vol. 1, no. 9, p. 1800066, 2018.

[52] T. Ohta, Y. Enomoto, J. L. Harden, and M. Doi, "Anomalous rheological behavior of ordered phases of block copolymers. 1," *Macromolecules*, vol. 26, no. 18, pp. 4928–4934, 1993.

[53] H. Kodama and M. Doi, "Shear-induced instability of the lamellar phase of a block copolymer," *Macromolecules*, vol. 29, no. 7, pp. 2652–2658, 1996.

[54] S. Latif, R. Mallah, and I. Soomro, "Discretization of laplacian operator in polar coordinates system on 9-point stencil with mixed pde's derivative approximation using finite difference method," *Journal of Mathematical Sciences & Computational Mathematics*, vol. 2, no. 3, pp. 387–394, 2021.

[55] M. Bahiana and Y. Oono, "Cell dynamical system approach to block copolymers," *Physical Review A*, vol. 41, no. 12, p. 6763, 1990.

[56] S. Chauhan, S. Mandal, V. Yadav, P. K. Jaiswal, M. Priya, and M. D. Shrimali, "Machine learning based prediction of phase ordering dynamics," *Chaos: An Interdisciplinary Journal of Nonlinear Science*, vol. 33, no. 6, 2023.

[57] I. W. Hamley, "Cell dynamics simulations of block copolymers," *Macromolecular theory and simulations*, vol. 9, no. 7, pp. 363–380, 2000.

[58] Y. Oono and S. Puri, "Study of phase-separation dynamics by use of cell dynamical systems. i. modeling," *Physical Review A*, vol. 38, no. 1, p. 434, 1988.

[59] T. Ohta and K. Kawasaki, "Equilibrium morphology of block copolymer melts," *Macromolecules*, vol. 19, no. 10, pp. 2621–2632, 1986.

[60] Y. Oono and S. Puri, "Computationally efficient modeling of ordering of quenched phases," *Physical review letters*, vol. 58, no. 8, p. 836, 1987.

[61] X. Guo, M. Pinna, and A. V. Zvelindovsky, "Parallel algorithm for cell dynamics simulation of block copolymers," *Macromolecular Theory and Simulations*, vol. 16, no. 9, pp. 779–784, 2007.

[62] I. A. Inayatullah Soomro, S. B. Shah, A. Majid, R. Muhammad, A. Hameed, G. Abas, A. V. Zvelindovsky, M. Pinna, and W. Ahmed, "Mathematical modelling of cylindrical forming di-block co-polymers confined in circular annular pores," *IJCSNS*, vol. 19, no. 2, p. 16, 2019.

[63] M. J. Iqbal, I. Soomro, M. Bibi, and R. N. Mallah, "Morphological investigation of lamellae patterns in diblock copolymers under change of thickness and confinement in polar geometry," *VFAST Transactions on Mathematics*, vol. 11, no. 2, pp. 174–197, 2023.

[64] M. J. Iqbal, I. Soomro, and U. Gulzar, "Patterns of nanoporous spherical packing emerging under influence of curvature and confinement," *VFAST Transactions on Mathematics*, vol. 12, no. 1, pp. 121–136, 2024.

[65] G. J. Papakonstantopoulos, K. C. Daoulas, M. Muller, and J. J. de Pablo, "Monte carlo simulation study of diblock copolymer self assembly," *arXiv preprint arXiv:1604.05265*, 2016.

[66] J. H. Ryu, H. S. Wee, and W. B. Lee, "Molecular dynamics study on microstructures of diblock copolymer melts with soft potential and potential recovery," *Physical Review E*, vol. 94, no. 3, p. 032501, 2016.

[67] P. Beránek, P. Posocco, and Z. Posel, "Phase behavior of gradient copolymer melts with different gradient strengths revealed by mesoscale simulations," *Polymers*, vol. 12, no. 11, p. 2462, 2020.